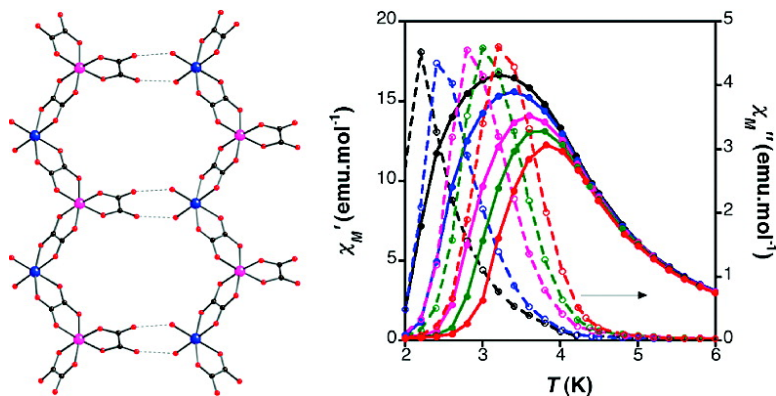


## Single Chain Magnets Based on the Oxalate Ligand

Eugenio Coronado, Jose# R. Gala#n-Mascaro#s, and Carlos Mart#-Gastaldo

*J. Am. Chem. Soc.*, **2008**, 130 (45), 14987-14989 • DOI: 10.1021/ja806298t • Publication Date (Web): 21 October 2008

Downloaded from <http://pubs.acs.org> on February 8, 2009



### More About This Article

Additional resources and features associated with this article are available within the HTML version:

- Supporting Information
- Access to high resolution figures
- Links to articles and content related to this article
- Copyright permission to reproduce figures and/or text from this article

[View the Full Text HTML](#)



**ACS Publications**  
 High quality. High impact.

## Single Chain Magnets Based on the Oxalate Ligand

Eugenio Coronado,\* José R. Galán-Mascarós, and Carlos Martí-Gastaldo

Universidad de Valencia, Instituto de Ciencia Molecular, Polígono de la Coma s/n,  
46980 Paterna, Spain

Received August 17, 2008; E-mail: eugenio.coronado@uv.es

Since the discovery of single-molecule magnets (SMMs) in 1993,<sup>1</sup> the synthesis and physical characterization of molecular nanomagnets has become one of the most active fields in molecular magnetism. Several aspects justify their importance: coexistence of classical properties attributed to bulk magnetic materials and quantum effects (quantum tunneling of the magnetization<sup>2</sup> and phase interference<sup>3</sup>), extremely long times for the relaxation of their magnetic moment and their potential use in molecular spintronics<sup>4</sup> and quantum computing.<sup>5</sup> Almost a decade later, Gatteschi et al. observed slow relaxation of the magnetization in a magnetically isolated cobalt(II) nitronyl nitroxide chain<sup>6</sup> and described the main experimental requirements to be fulfilled in the design of such 1D nanomagnets: strong uniaxial Ising-type anisotropy and high ratio between intra- ( $J$ ) and interchain ( $J'$ ) magnetic interactions. These magnetic nanowires were called single-chain magnets (SCMs),<sup>7</sup> by analogy to their 0D counterparts, and have attracted important attention since they might afford extended correlation lengths of the magnetization at comparatively higher temperatures.

Currently, one of the focuses of interest in this area is that of generating families of SCM-like compounds in which the anisotropy and the strength of the magnetic exchange interactions can be tuned at will. The systematic study of such families should provide insights for a detailed understanding of the parameters that affect the slow relaxation behavior. Nevertheless, probably because of synthetic difficulties, only two examples of such families are known.<sup>7a,8</sup> In view of the widely demonstrated versatility of the oxalate ligand ( $C_2O_4^{2-}$ ) in the design of whole families of molecule-based magnets<sup>9</sup> we considered it interesting to explore the possibility of obtaining oxalate-supported SCMs. Moreover, the use of this ligand in the design of such systems represents a challenging goal since it mediates a comparatively small intrachain magnetic exchange ( $J(\text{Co}^{\text{II}}\text{-ox-Cr}^{\text{III}}) \approx 1\text{--}2\text{ cm}^{-1}$ ),<sup>10</sup> thus hindering the fulfillment of the demanding requirements necessary to observe SCM behavior. Indeed, no oxalate-based molecular nanomagnet has been reported so far.

Here we describe the structure and magnetic properties of the first oxalate-based SCM.  $[\text{C}_{12}\text{H}_{24}\text{O}_6\text{K}]_{1/2}[(\text{C}_{12}\text{H}_{24}\text{O}_6)(\text{FC}_6\text{H}_4\text{NH}_3)]_{1/2}[\text{Co}(\text{H}_2\text{O})_2\text{Cr}(\text{ox})_3]$  (**1**) is composed of bimetallic  $\text{Co}^{\text{II}}\text{-ox-Cr}^{\text{III}}$  ferromagnetic Ising-like chains and exhibits slow relaxation of the magnetization at low temperatures.

**1** is prepared by slow diffusion of its components. It crystallizes in the monoclinic  $P21/m$  space group.<sup>11</sup> It is made up of alternated anionic (A) and cationic layers (B and C) in a repeating pattern  $\text{--ABACABAC--}$  (See Figure 1). The anionic layer (A) is built up by alternating bimetallic chains running on the  $ac$  plane. Along the chain, each  $[\text{Cr}(\text{ox})_3]^{3-}$  complex is connected to two  $\text{Co}(\text{H}_2\text{O})_2^{2+}$  ions through the oxalate linker and vice versa thus resulting in the formula:  $[\text{Co}(\text{H}_2\text{O})_2\text{-}$

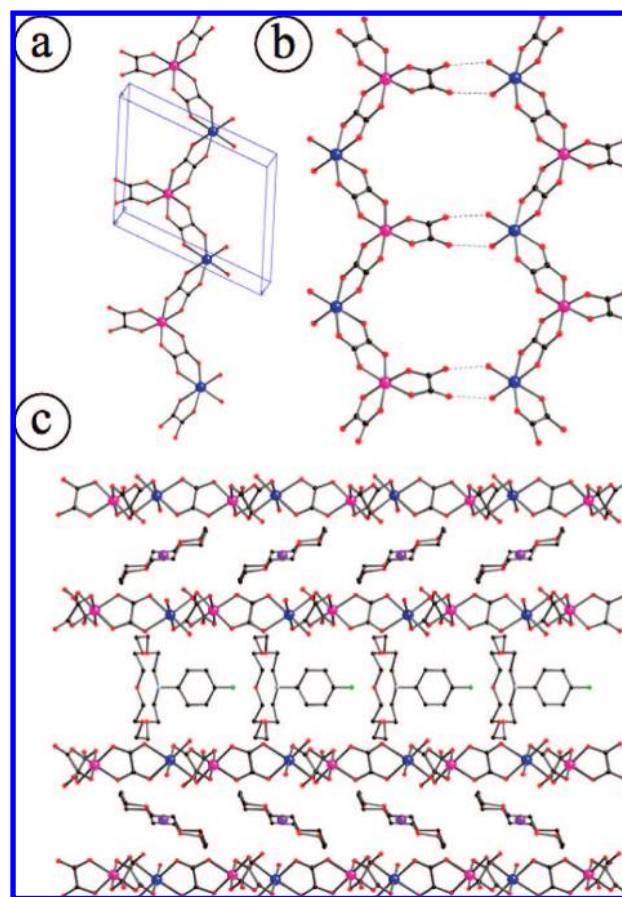


**Figure 1.** Three views of the crystal structure of **1**: (a) oxalate-bridged bimetallic chain; (b) 2D interactions of the chains through H-bonding in the  $ac$  plane; and (c) multilayered packing in the solid state.

$\text{Cr}(\text{C}_2\text{O}_4)_3]^-$  (intrachain  $\text{Co}^{\text{II}}\text{-Cr}^{\text{III}}$  distance  $5.33(1)\text{ \AA}$ ). Along the chains,  $\text{Cr}^{3+}$  ions adopt an octahedral coordination, with two bridging oxalate ligands in its bis-bidentate chelating form while the other acts as a terminal ligand. Minor distortion from regular octahedral geometry is observed for  $\text{Cr}^{3+}$  ions. Octahedral coordination is observed for  $\text{Co}^{2+}$  ions as well. Two  $\mu_2$ -oxalate bridging ligands and two water molecules in cis conformation surround each cobalt atom. As a consequence of its heteroleptic nature, higher distortion from regular octahedral geometry is observed for  $\text{Co}^{2+}$ . Adjacent chains are interlinked by the presence of hydrogen bonding interactions, which operate through the coordinating water molecules bonded to the  $\text{Co}^{2+}$  ions and the terminal oxalate ligand bonded to the  $\text{Cr}^{3+}$  atoms (shortest interchain  $\text{Co}^{\text{II}}\text{-Cr}^{\text{III}}$  distance  $7.62(1)\text{ \AA}$ ). The resultant assembled layer can be considered as a precursor of the classical

2D honeycomb network. (To confirm this point magnetic measurements were performed on **1** after gently heating, see Supporting Information, SI8.) Indeed, if the coordinated water molecules are eliminated, the oxalate terminal ligands transform into bridging ligands, thus generating the hexagonal network (See Figure 1b and Supporting Information). B cationic layers are composed by a pseudo-hexagonal packing of [K-(18-crown-6)]<sup>+</sup> complexes. The tilted orientation (ca. 28°) with respect to the anionic layers determines an interlayer separation of 9.15 Å. C cationic layers are composed of a pseudocubic arrangement of [(FPhNH<sub>3</sub>)-(18-crown-6)]<sup>+</sup> complexes. In this case, the crown ether mean plane is oriented perpendicularly (ca. 90°) with respect to the oxalate-based layer, thus forcing the anionic planes to remain more separated in the solid state (ca. 10.4 Å).

Static magnetic measurements were performed on grinded hand-collected crystals of **1**.  $\chi_M T$  product at room temperature is 6.63 emu.K.mol<sup>-1</sup> (see SI1). This value is bigger than that expected for the sum of two noninteracting Co<sup>2+</sup> ( $S_{Co} = 3/2$ ) and Cr<sup>3+</sup> ( $S_{Cr} = 3/2$ ) ions, probably induced by the presence of strong orbital contribution in octahedral Co<sup>II</sup>. As the system is cooled down  $\chi_M T$  product starts to increase smoothly down to 40 K where it becomes sharper, suggesting the presence of strong ferromagnetic intrachain interactions.  $\chi_M T$  reaches a maximum value of ca. 118.9 emu.K.mol<sup>-1</sup> K at 5.6 K, which corresponds to a steep jump in the  $\chi_M$  versus  $T$  plot (see SI1), suggesting the possibility of the onset of a long-range ordered or superparamagnetic state. The Curie–Weiss fitting of  $1/\chi_M$  in the high-temperature regime (50–300 K) yields a Curie constant value of 5.8 emu.K.mol<sup>-1</sup> and a  $\Theta$  value of 13.3 K (see SI2). The large positive  $\theta$  value confirms the presence of ferromagnetic exchange interactions, as typically mediated by the bis-bidentate oxalate ligand when bridging Co<sup>2+</sup> and Cr<sup>3+</sup> ions. The zero field-cooled magnetization defines a maximum at 3.2 K and diverges from the field-cooled curve at 5.6 K (see SI3). This irreversibility confirms the onset of a superparamagnetic state while the plateau observed for the FC magnetization below the blocking temperature accounts for the complete freezing process. Field dependence of the magnetization at 2 K constitutes an additional support of the ferromagnetic nature of the intrachain magnetic interaction (see SI4). Indeed, a rapid increase of the magnetization with the applied field is observed ( $M$  around 3.7  $\mu_B$  at 2 kOe). Saturation value (ca. 5  $\mu_B$ ) is slightly smaller than that expected for the perfect parallel alignment of the Co<sup>II</sup>–Cr<sup>III</sup> units. This fact might be induced by the presence of spin canting in the frozen ferromagnetic state as previously observed for other oxalate-based magnets. A hysteresis loop is observed at 2 K ( $H_c = 80$  Oe), confirming the magnet-like behavior of **1** (See SI5). Heat capacity measurements, performed on grounded crystals, corroborate the absence of 3D bulk magnetic ordering. Indeed, no  $\lambda$  peak was observed when cooling down to 2 K.

AC dynamic susceptibility measurements in the 1–1000 Hz interval under an oscillating field of 3.95 Oe show strong frequency dependence for both the in-phase ( $\chi_M'$ ) and out-of-phase ( $\chi_M''$ ) signals (Figure 2a).  $\chi_M'$  shows a maximum and starts to decrease in the 3.8–3 K range while  $\chi_M''$  defines a maximum in between 3.2 K (1000 Hz) and 2.2 K (1 Hz). To rule out the presence of glassiness, a quantitative measure of the frequency dependence was estimated with the frequency shift parameter first introduced by Mydosh.<sup>12</sup> The obtained  $\phi$  value (0.11) is in excellent agreement with that expected for superparamagnetic behavior ( $0.1 \leq \phi \leq 0.3$ ). This result is in agreement with the

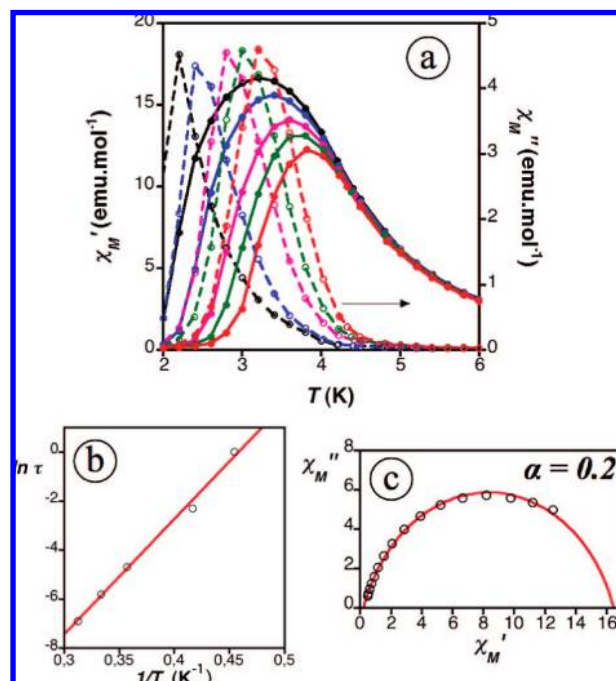


**Figure 2.** (a) In-phase (filled symbols) and out-of-phase (empty symbols) dynamic susceptibility of **1**. From left to right: 1, 10, 100, 332, and 1000 Hz. Solid lines are eye-guides. (b) Relaxation time fitting to the Arrhenius law in the 1–1000 Hz interval. (c) Cole–Cole plot at 2.5 K. Lines represent the best fitting of the experimental data to a Debye model providing  $\alpha = 0.2$ .

crystalline nature and the absence of competing magnetic interactions in **1**, both of them considered the main origins of glassy-behavior.<sup>13</sup> Moreover, as expected for a thermally activated Orbach process for the relaxation of the magnetization, frequency-dependence of  $\chi_M''$  maxima can be described by the Arrhenius law ( $\tau = \tau_0 \exp[\Delta/k_B T]$ ; where  $\tau$  is the relaxation time,  $\Delta$  is the effective energy barrier for the reversal of the magnetic moment,  $k_B$  is the Boltzmann constant, and  $T$  is the temperature; Figure 2b). Best fitting of the experimental data provides:  $\tau_0 = 4.4 \times 10^{-10}$  s and  $\Delta/k_B = 46.9$  K ( $R = 0.997$ ). These values are physically meaningful and in the range of the previously reported values for SMM and SCM systems.<sup>1,6–8</sup> For a better understanding of the dynamic properties of **1**, frequency dependence of  $\chi_M'$  and  $\chi_M''$  were studied at a fixed temperature in the Cole–Cole plot (see Figure 2c and SI7). The experimental data were fitted to a general Debye model in the 1–1000 Hz range.<sup>14</sup> The semicircle Cole–Cole diagram and the obtained  $\alpha$  value ( $\alpha = 0.2$ ;  $\alpha = 0$  for an infinitely narrow distribution of relaxation times) is in good agreement with that expected for superparamagnetic-like systems and indicates that the relaxation of the magnetization occurs nearly through a single process. Furthermore, temperature dependence of the correlation length in **1** was also studied (see SI6). As previously described for SCM systems,<sup>15</sup> an exponentially activated regime at high temperatures followed by saturation as the system was cooled down were observed.

In conclusion, compound **1** represents the first member of a series of isostructural oxalate-based compounds exhibiting tunable SCM-like properties. The synthetic versatility exhibited by the oxalate linker in the design of molecule-based magnets should permit an easy substitution of the metal ions consequently tuning the nature, extent, and anisotropy of the intrachain magnetic interactions. This work should result in the creation



of a complete family of SCM compounds that might provide important information concerning the main parameters that affect the slow-relaxation phenomena, which is a vital feature for the tuning and increasing of the blocking temperatures. In fact, preliminary results indicate that analogous bimetallic compounds (with  $M^{III} = \text{Fe, Mn, and Ru}$ ) can be prepared. We would like to note that although the ferromagnetic 1D-Ising chains are supramolecularly assembled through hydrogen-bonding interactions, the low efficiency of H bonding interactions to mediate magnetic exchange maintains the  $J'/J$  ratio small enough to observe the dynamic magnetic behavior of the single chains.<sup>16</sup> As a further matter, we note that the interchain distance in this material is similar and even shorter than those observed in other bimetallic oxalate-bridged 1D chains, where SCM behavior was not observed but bulk ferromagnetic ordering instead. The only difference in this case is the presence of a cationic layer, which leads to a larger separation between the magnetic layers, thus minimizing the effective interchain interactions between neighboring layers. In the examples exhibiting bulk magnetic properties, the insulation between adjacent layers was less efficient and subsequently the number of next-neighbors surrounding a given chain was higher. This observation suggests that the interlayer interaction might be key as well for the magnetism of these materials, even more important than in-plane direct interchain interactions. This suggests that longer interlayer distances could also promote SCM behavior in other analogous already known oxalate-bridged bimetallic chains and also in other 1D materials where the chains are supramolecularly arranged forming 2D networks.

**Acknowledgment.** Financial support from the European Union (NoE MAGMANet), the Spanish Ministerio de Ciencia e Innovación (Project Consolider-Ingenio in Molecular Nanoscience, CSD2007-00010, and projects MAT2004-03849 and MAT2007-61584), and the Generalitat Valenciana are gratefully acknowledged. We also acknowledge the help of J. M. Martínez-Agudo with the magnetic measurements.

**Supporting Information Available:** Crystal structure file in CIF format, detailed experimental procedure,  $\chi_M$  and  $\chi_M T$  vs  $T$  plots, Curie–Weiss fitting, FC and ZFC magnetizations, field dependence of the magnetization, hysteresis curve,  $\ln(\chi_M' T)$  vs  $1/T$  plot, Cole–Cole plots at 2.4, 2.3, and 2.2 K, and study of the thermal treatment effect on the magnetic properties of **1**. This material is free of charge via the Internet at <http://pubs.acs.org>.

## References

- (1) (a) Sessoli, R.; Gatteschi, D.; Caneschi, A.; Novak, M. A. *Nature* **1993**, *365*, 141–143. (b) Gatteschi, D.; Sessoli, R.; Villain, J. *Molecular Nanomagnets*; Oxford University Press: Oxford, 2006.
- (2) (a) Thomas, L.; Lioni, F.; Ballou, R.; Gatteschi, D.; Sessoli, R.; Barbara, B. *Nature* **1996**, *383*, 145–147. (b) Friedman, J. R.; Sarachik, M. P.; Tejada, J.; Ziolo, R. *Phys. Rev. Lett.* **1996**, *76*, 3830–3833.
- (3) Wernsdorfer, W.; Sessoli, R. *Science* **1999**, *284*, 133–135.
- (4) Bogani, L.; Wernsdorfer, W. *Nat. Mater.* **2008**, *7*, 179–186.
- (5) (a) Leuenberger, M. N.; Loss, D. *Nature* **2001**, *410*, 789–793. (b) Lehmann, J.; Gaita-Arino, A.; Coronado, E.; Loss, D. *Nat. Nanotechnol.* **2007**, *2*, 312–317.
- (6) Caneschi, A.; Gatteschi, D.; Lalioti, N.; Sangregorio, C.; Sessoli, R.; Venturi, G.; Vindigni, A.; Rettori, A.; Pini, M. G.; Novak, M. A. *Angew. Chem., Int. Ed.* **2001**, *40*, 1760–1763.
- (7) (a) Clérac, R.; Miyasaka, H.; Yamashita, M.; Coulon, C. *J. Am. Chem. Soc.* **2002**, *124*, 12837–12844. (b) Coulon, C.; Miyasaka, H.; Clérac, R. *Struct. Bonding (Berlin)* **2006**, *122*, 163–206.
- (8) Bernot, K.; Bogani, L.; Caneschi, A.; Gatteschi, D.; Sessoli, R. *J. Am. Chem. Soc.* **2006**, *128*, 7947–7956. Bernot, K.; Bogani, L.; Sessoli, R.; Gatteschi, D. *Inorg. Chim. Acta* **2007**, *360*, 3807.
- (9) See for example: (a) Tamaki, H.; Zhong, Z. J.; Matsumoto, N.; Kida, S.; Koikawa, M.; Achiwa, N.; Hashimoto, Y.; Okawa, H. *J. Am. Chem. Soc.* **1992**, *114*, 6974–6979. (b) Min, K. S.; Miller, J. S. *Dalton Trans.* **2006**, 2463–2467. (c) Coronado, E.; Galán-Mascarós, J. R.; Martí-Gastaldo, C. *J. Mater. Chem.* **2006**, *16*, 2685–2689. (d) Decurtins, S.; Schmalte, H. W.; Schneuwly, P.; Enslin, J.; Gutlich, P. *J. Am. Chem. Soc.* **1994**, *116*, 9521–9528. (e) Coronado, E.; Galán-Mascarós, J. R.; Gómez-García, C. J.; Martínez-Agudo, J. M. *Inorg. Chem.* **2001**, *40*, 113–120.
- (10) (a) Ohba, M.; Tamaki, H.; Matsumoto, N.; Okawa, H. *Inorg. Chem.* **1993**, *32*, 5385–5390. (b) Coronado, E.; Galán-Mascarós, J. R.; Giménez-Saiz, C.; Gómez-García, C. J.; Ruiz-Pérez, C. *Eur. J. Inorg. Chem.* **2003**, 2290–2298.
- (11) A purple prismatic crystal of **1** was collected by hand and mounted on a Nonius-Kappa CCD single crystal diffractometer using graphite-monochromated Mo  $K\alpha$  radiation ( $\lambda = 0.71073 \text{ \AA}$ ) at 110 K. Data collection was performed by using the program Collect.<sup>11</sup> Data reduction and cell refinement were performed with the programs Denzo and Scalepack. Crystal structure was solved by direct methods using the program SIR97, followed by Fourier synthesis and refined on  $F^2$  with Shelxl-97. Anisotropic least-squares refinement of non-H atoms was performed. All hydrogen atoms were located geometrically. All crystallographic plots were obtained via the CrystalMaker program.  $\text{H}_{55}\text{C}_{42}\text{Cr}_7\text{KCo}_2\text{FNO}_{40}$ ,  $M_w = 1493.83$ , monoclinic,  $P21/m$ ,  $a = 8.9240(2) \text{ \AA}$ ,  $b = 36.6840(11) \text{ \AA}$ ,  $c = 11.4110(3) \text{ \AA}$ ,  $\beta = 112.710(2)^\circ$ ,  $V = 3446.0(2) \text{ \AA}^3$ ,  $T = 110(2) \text{ K}$ ,  $Z = 2$ ,  $\rho_{\text{calc}} = 1.44 \text{ g/cm}^3$ ,  $F(000) = 1528$ ,  $\rho = 0.935 \text{ mm}^{-1}$ , 10835 reflections, 6690 unique ( $R_{\text{int}} = 0.0656$ ),  $2\theta_{\text{max}} = 53.42^\circ$ ,  $R(F) = 0.0665$  and  $R_w(F2) = 0.1580$  for 6690 reflections [ $I > 2s(I)$ ]. CCDC-691981 contains supplementary crystallographic data.
- (12) Mydosh, J. A. *Spin Glasses: An experimental introduction*; Taylor & Francis: London, 1993.
- (13) (a) Sellers, S. P.; Korte, B. B.; Fitzgerald, J. P.; Reiff, W. M.; Yee, G. T. *J. Am. Chem. Soc.* **1998**, *120*, 4662–4670. (b) Clérac, R.; O’Kane, S.; Cowen, J.; Ouyang, X.; Heintz, R.; Zhao, H.; Bazile, M. J., Jr.; Dunbar, K. R. *Chem. Mater.* **2003**, *15*, 1840–1850.
- (14) (a) Cole, K. S.; Cole, R. H. *J. Chem. Phys.* **1941**, *9*, 341–351. (b) Dekker, C.; Arts, A. F. M.; Dewijn, H. W.; Vanduyneveldt, A. J.; Mydosh, J. A. *Phys. Rev. B* **1989**, *40*, 11243–11251.
- (15) (a) Coulon, C.; Clérac, R.; Lecren, L.; Wernsdorfer, W.; Miyasaka, H. *Phys. Rev. B* **2004**, *69*, 132408. (b) Bogani, L.; Sessoli, R.; Pini, M. G.; Rettori, A.; Novak, M. A.; Rosa, P.; Massi, M.; Fedi, M. E.; Giuntini, L.; Caneschi, A.; Gatteschi, D. *Phys. Rev. B* **2005**, *72*, 064406. (c) Li, X. J.; Wang, X. Y.; Gao, S.; Cao, R. *Inorg. Chem.* **2006**, *45*, 1508–1516.
- (16) (a) Veciana, J.; Cirujeda, J.; Rovira, C.; Vidal-Gancedo, J. *Adv. Mater.* **1995**, *7*, 221–225. (b) Cirujeda, J.; Mas, M.; Molins, E.; Lanfranc de Panthou, F.; Laugier, J.; Park, J. G.; Paulsen, C.; Rey, P.; Rovira, C.; Veciana, J. *J. Chem. Soc., Chem. Commun.* **1995**, 709–710. (c) Romero, F. M.; Ziessel, R.; Bonnet, M.; Pontillon, Y.; Ressouche, E.; Schweizer, J.; Delley, B.; Grand, A.; Paulsen, C. *J. Am. Chem. Soc.* **2000**, *122*, 1298. (d) Coronado, E.; Galán-Mascarós, J. R.; Martí-Gastaldo, C. *Inorg. Chim. Acta* **2008**, *361*, 4017–4023.

JA806298T